Suresh Annam, Gopinadhanpillai Gopakumar, C.V.S. Brahmmananda Rao, N. Sivaraman, Akella Sivaramakrishna and Kari Vijayakrishna*

Experimental and theoretical studies on extraction of actinides and lanthanides by alicyclic H-phosphonates

Abstract: Three different alicyclic substituents H-phosphonates, namely, dicyclopentyl H-phosphonate, dicyclohexyl H-phosphonate and dimenthyl H-phosphonate were synthesized and used for liquid–liquid extraction of actinide elements (U, Am and Th) and lanthanide (Gd) in n-dodecane from nitric acid medium. The physicochemical properties of the extractants, such as density, viscosity, solubility were determined. At lower acidities, these H-phosphonates exhibit higher distribution values and the extraction following cation exchange mechanism through P–OH group of tri-coordinated phosphite form. At higher acidities (2N), the extraction is primarily via solvation mechanism through P=O group of penta-coordinated phosphonate form. Amongst the three H-phosphonates, examined dimenthyl H-phosphonate showed the best results for the actinide extraction. Density functional theory (DFT) calculations were applied to understand the electronic structure of the ligands and the metal complexes. The calculated large complexation energy of $UO_2(NO_3)_2 \cdot 2DMnHP$ is in agreement with the observed trend in experimental distribution ratio data.

Keywords: H-phosphonates, dialkyl H-phosphonate, actinides, lanthanides, liquid–liquid extraction, DFT calculations.

*Corresponding author: Kari Vijayakrishna, Department of Chemistry, School of Advanced Sciences, VIT University, Vellore 632014, Tamil Nadu, India, Tel.: +91 416 224 2334, Fax: +91 416 224 3092, E-mail: kari@vit.ac.in; vijayakrishnakari@gmail.com
Suresh Annam and Akella Sivaramakrishna: Department of Chemistry, School of Advanced Sciences, VIT University, Vellore 632014, Tamil Nadu, India
Gopinadhanpillai Gopakumar, C.V.S. Brahmmananda Rao and N. Sivaraman: Chemistry Group, Indira Gandhi Centre for Atomic Research (IGCAR), Kalpakkam 603102, Tamil Nadu, India

1 Introduction

Among various chelating molecules, organophosphorous compounds have been widely applied in hydrometallurgical and nuclear industrial processes for the extraction of lanthanides, actinides and various fission products from the irradiated nuclear fuel [1]. A variety of extraction processes were adopted for separation of actinides, which include precipitation [2], co-precipitation [3] and ion-exchange chromatography methods [4]. Among various methods, solvent extraction technique has been proved to be one of the most efficient processes for extraction and purification of actinides. Over the years, various kinds of organophosphorous extractants, namely, acidic [5, 6] neutral [7, 8] and basic [9] extractants have been investigated for actinide separation. Among these, neutral organophosphorous extractant, tri-n-butyl phosphate (TBP) has been used for the recovery of Pu from spent fuel by the PUREX [10] process and octyl(phenyl)-N,N-diisobutylcarbamoylmethylphosphine oxide (OØ-CMPO) is regarded as one of the ligands for extraction of trans-uranium elements and has been used in TRUEX [11] process.

Diesters of phosphonic acid (H_3PO_3), referred to as dialkyl H-phosphonates (dialkyl phosphite) are a class of organophosphorous compounds, contain a characteristic H–P=O structural motif, which governs their unique chemical properties. Dialkyl H-phosphonates have richer chemistry than their phosphate analog because of the presence of number of functional groups in the molecule (P–OR, P–H and P=O). It is due to these unique chemical properties, H-phosphonates and their derivatives have growing applications in agrochemicals, medicinal compounds [12] and synthons in many organo-catalytic reactions [13, 14].

In the present work, we have investigated the role of substituents in alicyclic H-Phosphonates on the extraction behavior of actinides and lanthanides. In this regard, some of the compounds of this family have been synthesized and studies have been reported [15]. The present study involves synthesis, characterization of three compounds of H-phosphonate bearing alicyclic substituents.

In order to understand the role of structure on the extraction behavior of these compounds, theoretical investigations were carried out by applying DFT methodologies.

2 Experimental

2.1 Materials and instrumentation

Phosphorus trichloride, cyclopentanol, cyclohexanol, l-menthol, Arsenazo-I and Arsenazo-III were procured from SD Fine chemicals. The solvent/diluents, *n*-dodecane was purchased from Fluka. The Hydrated metal salts (Loba and Aldrich, India), [Th(NO$_3$)$_4$·5H$_2$O)] and [Gd(NO$_3$)$_3$·6H$_2$O)] were used as received. The actinides, [241]Am and [233]U tracers were used from laboratory stock solutions and their radiochemical purity was established prior to use. All other chemicals used for synthesis and other experimental work were of reagent grade and used without further purification.

The ^{1}H, ^{13}C, and ^{31}P{^{1}H}-NMR spectra were recorded using BRUKER DMX-400 and all ^{1}H chemical shifts were reported relative to the residual proton resonance in deuterated solvents (all at 25°C, CDCl$_3$)·H$_3$PO$_4$ was used as an external standard for ^{31}P {^{1}H}-NMR. CHN analysis was carried out by Vario EL elemental analyzer. FT-IR spectra were recorded on SHIMADZU Affinity-1 FT-IR spectrometer with KBr pellet. UV–Vis absorption spectra were recorded with using SHIMADZU UV-3600 double-beam spectrophotometer. Total organic carbon (TOC) analysis was carried out by Analytikjena/multi N/C 3100 TOC analyzer.

2.2 Synthesis of alicyclic H-phosphonates

The H-phosphonate derivatives were synthesized as per the procedure described below (Scheme 1).

2.2.1 General procedure

Alicyclic H-phosphonates **1a−c** were synthesized according to the modified literature report [16]. For instance,

phosphorus trichloride (0.364 mol) and dichloromethane (100 mL) were placed in a 500 mL flask in an ice bath, equipped with a magnetic stirrer and a guard tube. The corresponding alcohol (1.092 mol) diluted with dichloromethane (100 mL) was added drop-wise to the precedent mixture. The mixture was stirred for 2 h at room temperature. Subsequently, the reaction mixture was further diluted with dichloromethane and washed with saturated solution of sodium carbonate, water and the organic phase was concentrated under reduced pressure to afford an alicyclic hydrogen phosphonates as colorless liquids. The crude products were purified to remove the unreacted alcohols and alkyl chlorides formed in the course of reaction by silica gel column chromatography using a mixture of 30% ethyl acetate and petroleum ether as eluent.

2.3 Physicochemical properties

### 2.3.1 Solubility of H-phosphonates in water

An equal volume of extractants and distilled water were equilibrated for 12 h. The biphasic solution was allowed to settle down and the aqueous layer was analyzed for the total organic content using total organic carbon analyzer and the solubility of H-phosphonates was determined.

2.3.2 Density measurements

The density of the neat samples was measured in triplicate by weighing 500 μL of the sample in a glass micropipette at room temperature.

2.3.3 Viscosity measurements

The viscosity of H-phosphonates was measured by Oswald viscometer [17]. A known volume (~ 15 mL) of liquid was taken in a viscometer and the time taken by the liquid to flow through the marked region of the Oswald viscometer was measured as a function of temperature. The driving pressure *p* at all stages of the flow of a liquid is given by
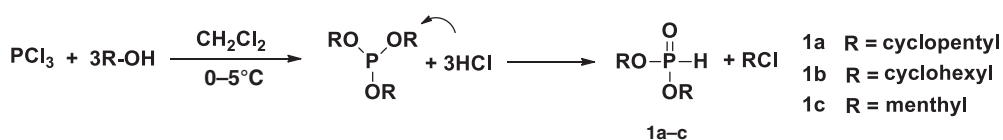
Scheme 1: Synthesis of alicyclic H-phosphonates.

$h\rho g$, where h is the difference in the heights of the liquid in upper and lower bulb, ρ the density of the liquid and g the acceleration due to gravity. The viscosity of the fluid of interest can be determined using the following expression.

$$\eta_{f} = \eta_{w}(\rho_{f} t_{f}/\rho_{w} t_{w}) \tag{1}$$

where η_{f}, ρ_{w} and t_{f} are the viscosity, density and time taken for the fluid to pass through marked region of the viscometer of fluid to be determined. η_{w}, ρ_{w} and t_{w} are viscosity, density and time for the water system under identical conditions.

2.4 Radiometric assay

Radiometric assay of [233]U was carried out using a liquid scintillation counting technique using a LSC system (Hidex, Finlad) coupled to a multi-channel analyzer using a dioxane-based scintillator cocktail [18]. [241]Am was assayed by a well-type Na(Tl) scintillation counter coupled to a multi-channel analyzer (ECIL, India).

2.5 Distribution measurements

2.5.1 Uranium and Americium

Solutions of desired concentration of H-phosphonates were prepared in *n*-dodecane and equilibrated (2 mL) with an equal volume of aqueous phase (containing requisite quantity of [233]U/[241]Am tracer) in a rotary thermostated water bath for 60 min at 298 K. After attainment of equilibrium, suitable aliquots from the both the phases (e. g. 100 µL) were taken for radiometric assay of the actinides. The distribution ratio (D_M) was calculated as the ratio of concentration (radioactivity per unit volume per unit time) of metal ions in the organic phase to that in the aqueous phase

$$D_{M} = \frac{[M]_{org}}{[M]_{aq}} \tag{2}$$

where $[M]_{org.}$ and $[M]_{aq.}$ are the metal ion concentration in the organic and aqueous phases, respectively.

2.5.2 Thorium and Gadolinium

The experimental procedure used for the extraction of Th(IV) and Gd(III) was similar to that of uranium extraction. The initial concentration of thorium and gadolinium

[5×10⁻⁴ M] in the aqueous phase as well as at the equilibrium was determined spectrophotometrically using Arsenazo-III and Arsenazo-I as a chromogenic agent, respectively. The distribution ratios for non-radioactive metal ions were calculated by analyzing the aqueous phase before ($[M]_{I,aq.}$) and after ($[M]_{f,aq.}$) contact with the organic phase. Assuming no losses to sorption or precipitation and no changes in the phase volumes, the difference between $[M]_{I,aq.}$ and $[M]_{f,aq.}$ defines the concentration of metal in the organic phase. The distribution ratio can then be defined as

$$D_{M} = \frac{[M]_{i,aq} - [M]_{f,aq}}{[M]_{f,aq}} \tag{3}$$

All the batch sorption studies were performed in nitric acid media ranging from 0.01 M to 6 M and experiments were carried out in triplicate.

2.6 Computational methodologies

DFT calculations were applied to investigate the electronic structure and geometries of dicyclopentyl, dicyclohexyl and dimethyl H-Phosphonates, and their respective complexes with $UO_2(NO_3)_2$. The ligand geometries were optimized employing the hybrid B3LYP functional [19, 20] in conjunction with triple-ζdef2-TZVP basis sets [21, 22]. The former functional is expected to provide reasonably good geometries and energies for organic molecules [23, 24]. The located stationary points were characterized as energy minima on the potential energy hypersurface, by performing harmonic vibrational frequency calculations at the same level. The resolution-of-identity (RI) approximation was applied in conjunction with the appropriate auxiliary basis sets for fast computations [25–27]. It is to be noted that, even though dispersion interactions are weak for one pair of interacting atoms, it will be significant in the case of large structures due to the increase in the number of pairwise interactions present in those systems. In order to account for the dispersion effects, empirical Grimme-type dispersion corrections were incorporated during this step using the latest atom-pairwise dispersion correction with Becke-Johnson damping (D3BJ) [28, 29]. Increased integration grids (Grid6 in ORCA convention) and tight SCF convergence criteria were used throughout the calculations. On the other hand, for the calculation of uranium metal complexes, the hybrid density functional PBE0 [30], with 25% HF exchange, was employed and tight SCF convergence criteria was used throughout the calculations. It is reported that PBE0 + D3 combination give very good

description of geometries for uranium complexes [31]. For Uranium atom, the 60 inner-shell core electrons were replaced by an effective core potential (ECP) generated for the neutral atom using quasi-relativistic methods [32–34], and the explicitly treated electrons were described by the standard def2-TZVP basis sets. This basis set combination is referred to hereafter as def2-TZVP-ECP and was adopted for previous theoretical calculations of uranium complexes, where the results showed good agreement with experiment [31]. All quantum chemical calculations were performed with ORCA version 3.0.3 program package [35].

3 Results and discussion

3.1 Characterization of extractants

The derivatives of diesters of phosphonic acid bearing alicyclic substituents (H-phosphonates, Figure 1), namely dicyclopentyl H-phosphonate (DCyPeHP), dicyclohexyl H-phosphonate (DCyHeHP) and dimenthyl H-phosphonate (DMnHP), were synthesized as per the literature [16] and characterized using FT-IR, NMR (^{1}H, ^{31}P{^{1}H} and ^{13}C) and elemental analysis (Table 1).

The proton coupled ^{31}P NMR spectra of compounds **1a−c** shows two signals at δ 2.0–6.0 ppm (Figure 2) for the corresponding P=O with coupling constant $^1J_{PH} = 663$, which is the characteristic environment of the P atom. The structures of the compounds obtained were confirmed by ^{1}H NMR spectra, which shows characteristic sets of signals

for corresponding substituents at the P–O–R and P–H protons, signals for P–H proton at δ 6.0–7.7 (Figure 3) as a doublet ($J = 688$ Hz).

The IR spectra of the H-phosphonates show characteristic absorption bands attributed to stretching frequencies of P–H, P=O and bending frequency of P–O–C. The P–H stretch uniquely placed in the range of 2300–2500 cm^{-1} and is characteristic of H-phosphonates and usually unoccupied by the bands of interfering groups. The P=O and P–H stretching frequencies of all the H-phosphonates (Table 1) are comparable with the literature reports [36].

3.2 Viscosity

Viscosity is an important parameter that decides the mass transfer property from aqueous to the organic phase. Low viscosity is preferred since high viscosity resist mass-transfer and makes liquid-liquid phase separation difficult. Sometimes an extraction process is operated at an elevated temperature where viscosity is significantly lower for better mass transfer even if the distribution ratios are relatively lower.

If the coefficient of viscosity, η_1, of a standard liquid is known, the coefficient, η_2, of second liquid may be determined from

$$\eta_2/\eta_1 = (\rho_2 t_2)/(\rho_1 t_1) \tag{4}$$

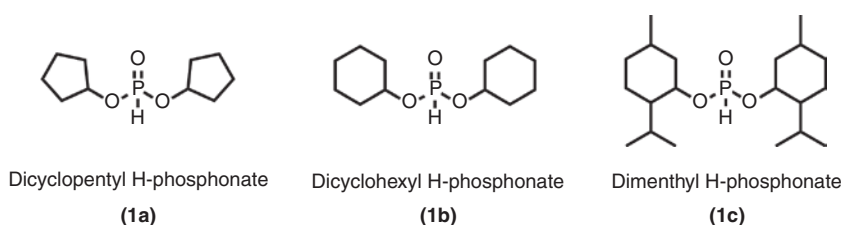where t_2 and t_1 are the measured time of flow of equal volumes of the two liquids through the same viscometer.

Dicyclopentyl H-phosphonate	Dicyclohexyl H-phosphonate	Dimenthyl H-phosphonate
(1a)	**(1b)**	**(1c)**

Figure 1: Chemical structures of the compounds used in this study.

Table 1: Physiochemical properties of alicyclic H-phosphonates.

Compound	Density (g/mL) T=298 K	Viscosity (cP) (T=298 K)	Solubility (mg/L) (T=298 K)	IR (cm⁻¹)	Elemental composition
Dicyclopentyl H-phosphonate (DCyPeHP)	1.076	2.76	2810	P=O (1250) P–H (2424)	C– 67.88% H– 10.18%
Dicyclohexyl H-phosphonate (DCyHeHP)	1.062	3.18	2180	P=O (1250) P–H (2424)	C– 58.10% H– 9.69%
Dimenthyl H-phosphonate (DMnHP)	0.960	11.74	767.9	P=O (1250) P–H (2424)	C– 55.48% H– 8.62%

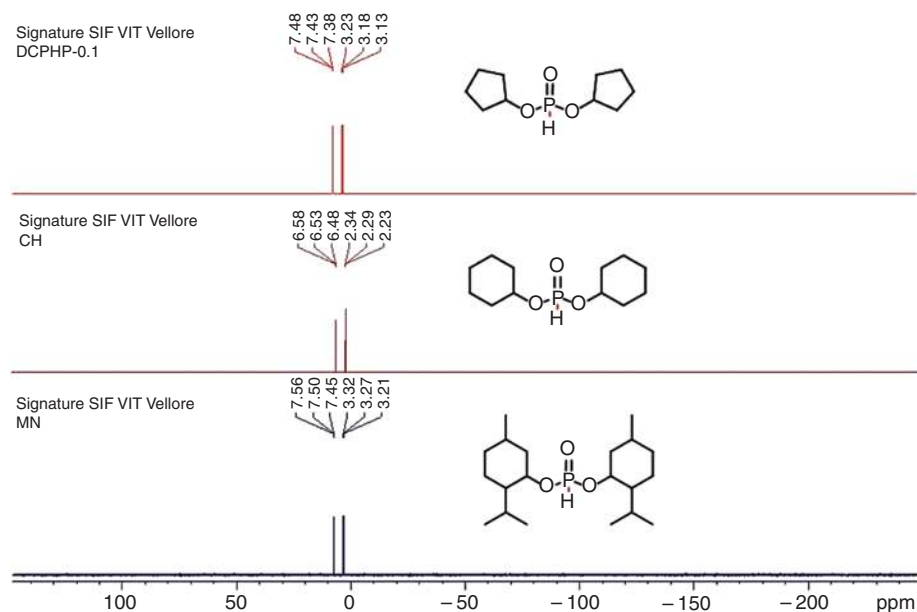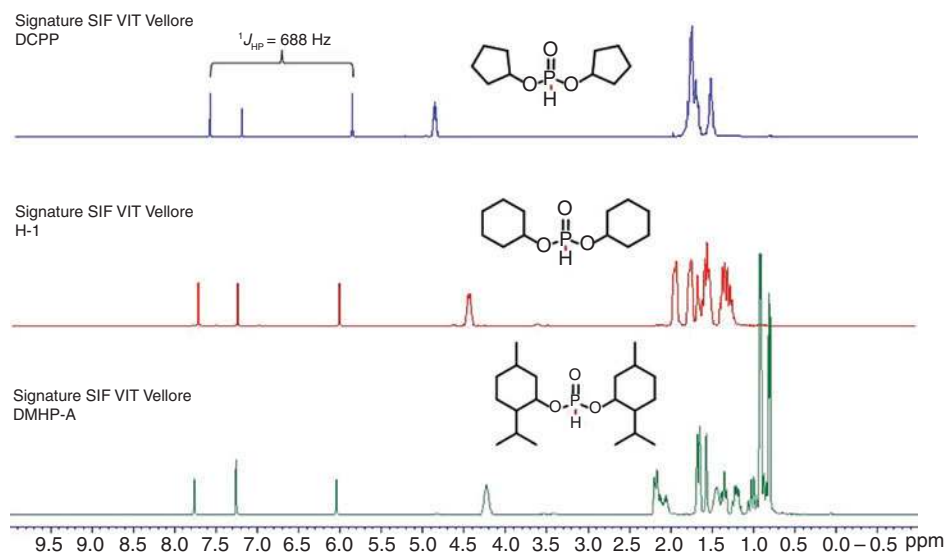**Figure 2:** ^{31}P-NMR overlay spectra of three synthesized H-phosphonates.

Figure 3: ^{1}H-NMR overlay spectra of three synthesized H-phosphonates.

The variation of viscosity of H-phosphonates as a function of temperature is shown in Figure 4. The relative standard deviation for the measurement of viscosity by Oswald viscometer is 1–2%. The deviations can be maximum at higher temperatures due to the error incorporated because of the assumption of invariance in density as a function of temperature. In the case of water, the density at 298 K and 323 K is 0.997 and 0.988 g/mL, respectively. This corresponds to an uncertainty of 1% in the calculation of viscosity by this method. As seen from the Figure 4, the viscosity decreases with increase in temperature. This is due to the energy available to the molecules to overcome the resistance to flow, caused by the reduction in the interactions among the molecules. The effect of temperature on the viscosity can be fitted with the Arrhenius type of relationship as shown in Eq. 5
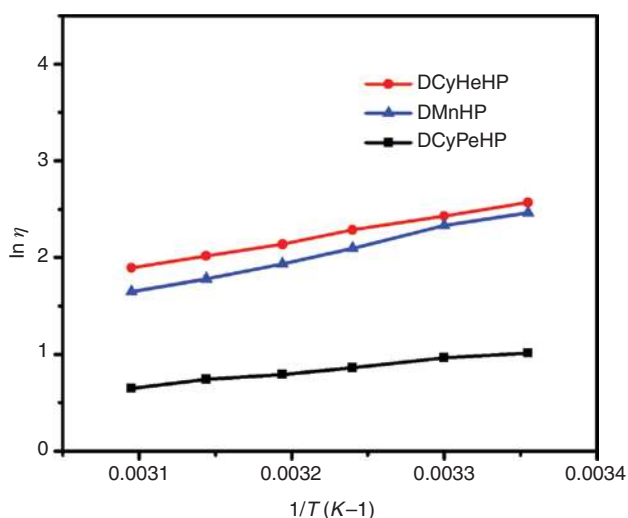
$$\eta = \eta_0 e^{E_\alpha / RT} \tag{5}$$

where η_0 is dynamic viscosity (Pa·s); η is the pre-exponential factor (Pa·s); E_α is the exponential constant which
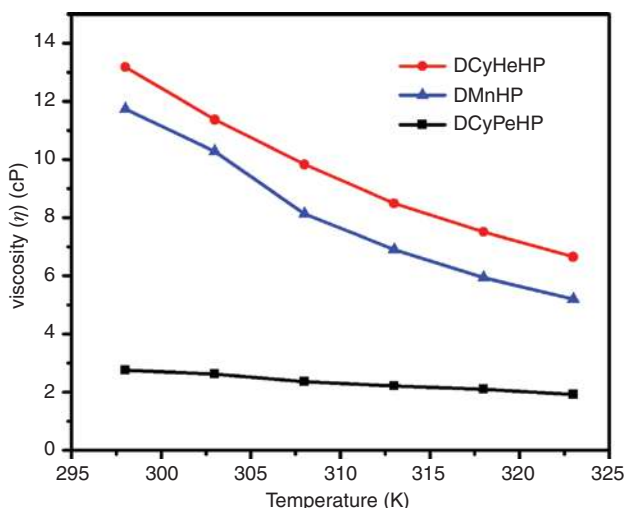
Figure 4: Variation of viscosity of H-phosphonates as a function of temperature.

is known as activation energy (J/mol); R is the gas constant (J/mol/K) and T is the absolute temperature (K). The plot of $\ln\eta$ against $1/T$ for H-phosphonates is shown in Figure 5. At 303 K, the (calculated from the slope of the straight lines) values for **1a**, **1b** and **1c** are 11.68, 21.84 and 27.01 kJ/mol, respectively. The activation energy increases with the increase in the size of the extractant because as molecular size increases, the Vander Waals forces operating among the molecules also increases there by necessitating higher energy to overcome the resistance to flow of extractants.

3.3 Distribution studies

3.3.1 Uranium and Thorium

The distribution studies of uranium (VI) with 0.5 M solutions of H-phosphonates in n-dodecane from nitric acid media, 0.01–6 M is shown in Figure 6. These results show the dependence of the distribution ratio $D_{U(VI)}$ with increasing nitric acid concentration, i. e. passes through a maximum at 0.01 M nitric acid concentration. Higher distribution for uranium was observed at lower acidity (Figure 6). As the nitric acid concentration increases from 0.1–1 M, a decrease in D values was observed, this is in agreement with the data of Das et al. [37]. Furthermore, the D values do not show much variation from 2 to 6 M nitric acid. The decrease in extraction of uranium with increase in feed acidity is in accordance with the cation exchange behavior.
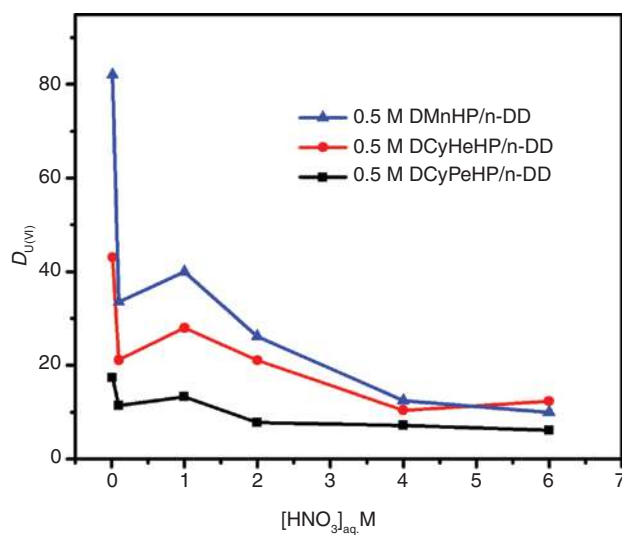
$$nRPO-H+mM^{n+}_{aq} \rightarrow RPO-M\ org.+nH^{+}_{aq} \tag{6}$$
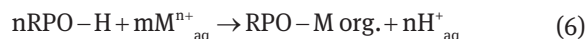
where RPO–H is the tri-coordinated phosphite form in equilibrium with penta-coordinated H-phosphonate form (Figure 7), where H is exchangeable as in acidic extractants.
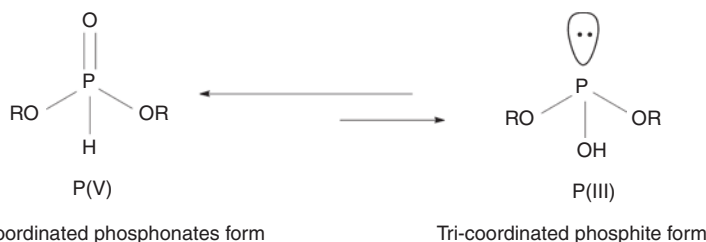
The equilibrium constant K_{eq}, for the reaction is given by

$$K_{eq} = [RPO-M]_{org.}\ [H^{+}]^{n}/[RPO-H]^{n}[M]^{n+}_{aq} \tag{7}$$

Rearranging Eq. (7),

Figure 5: Arrhenius plot for the variation of viscosity with temperature for H-phosphonates.

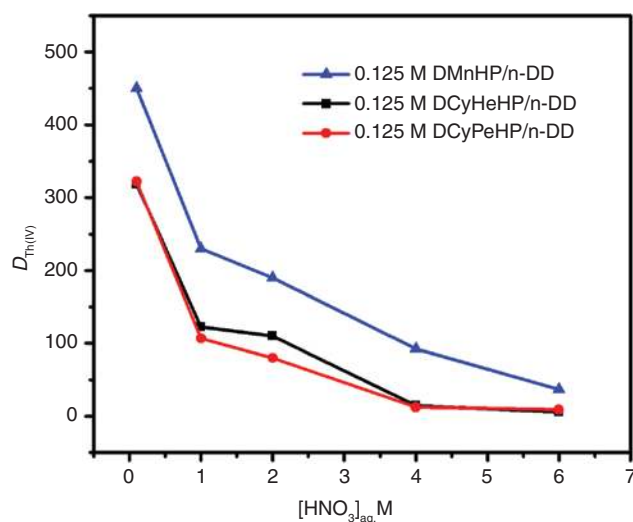**Figure 6:** Variation of $D_{U(VI)}$ with equilibrium aqueous phase nitric acid for the H-phosphonates at 303 K.

Figure 7: Tautomeric equilibrium in H-phosphonates.

$$D = K_{eq}[RPOH]^n / [H^+]^n \qquad (8)$$

The above equations clearly indicate that the degree of extraction is strongly dependent on hydrogen ion concentration. Throughout the nitric acid concentration, at lower acidity, the uranium extraction takes place by cation exchange and at higher acidity, the extraction was primarily through solvation mechanism.

Figure 8 shows the effect of HNO_3 concentration in the equilibrium aqueous phase on the extraction of Th(IV) ions with solutions of compound **1a−c** in *n*-dodecane. The distribution ratios of Th(IV) from 0.01 to 6 M HNO_3 was measured with 0.125 M H-phosphonates in *n*-dodecane. The concentration of extractant of H-Phosphonate was limited to 0.125 M as the concentration in the aqueous values for Th(IV) were below the detection limit in the spectrophotometric method of analysis in case extractant concentration was kept above 0.125 M. An increase in HNO_3 concentration is accompanied by the steep decrease in distribution ratios of Th(IV) up to 1 M. The decrease in *D* values is gradual with DMnHP from 1 to 6 M nitric acid concentration. In case of DcyPeHP and DCyHeHP the reduction in *D* values
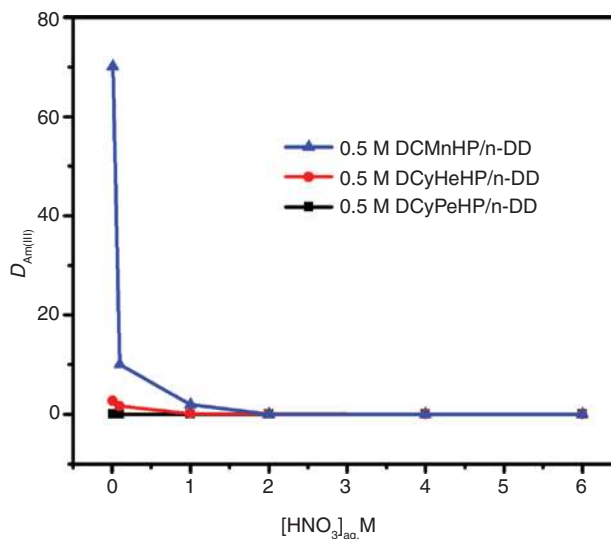
is steep until 4 M nitric acid concentration followed by a plateau from 4 to 6 M nitric acid concentration.

### 3.3.2 Americium and Gadolinium

Figures 9 and 10 shows the extraction of Am and Gd as a function of nitric acid concentration with 0.5 M H-phosphonates (**1a−c**) in *n*-dodecane medium. This extraction of Am(III) and Gd(III) is extremely low compared to U(VI) and Th(VI) systems for all the H-Phosphonates. Interestingly the menthyl system shows a higher distribution at lower acidity (0.01 M) compared to other H-Phosphonates. The phosphoryl groups in these compounds does not extract Am(III) at higher acidities.

3.4 Density functional theory studies

We have applied DFT calculations to understand the electronic structure of the ligands, DCyPeHP, DCyHeHP

Figure 8: Variation of $D_{Th(IV)}$ with equilibrium aqueous phase nitric acid for the H-phosphonates and at 303 K.

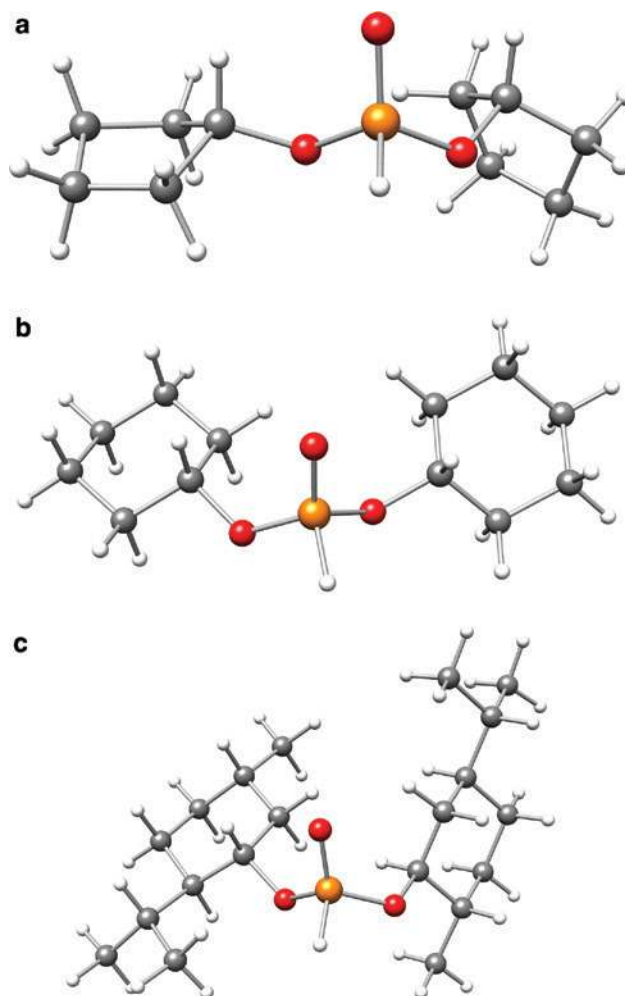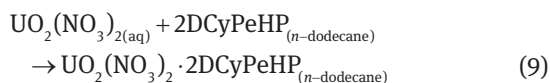**Figure 9:** Variation of $D_{Am(III)}$ with equilibrium aqueous phase nitric acid for the H-phosphonates at 303 K.
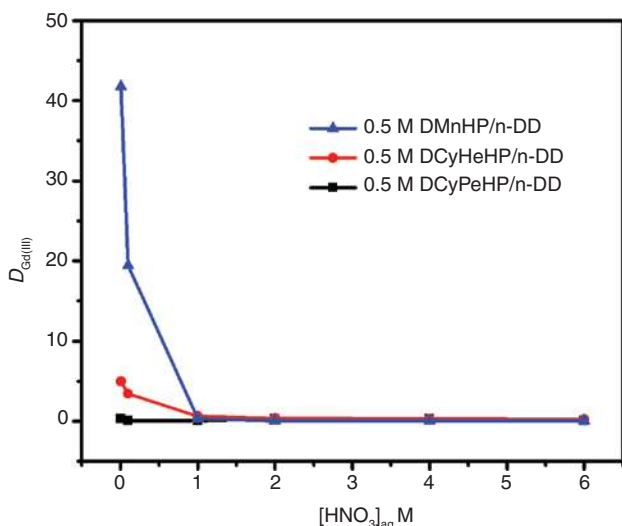
Figure 10: Variation of $D_{Gd(III)}$ with equilibrium aqueous phase nitric acid for the H-phosphonates at 303 K.

Figure 11: Optimized geometries of (a) dicyclopentyl H-phosphonate (DCyPeHP), (b) dicyclohexyl H-phosphonate (DCyHeHP), and (c) dimenthyl H-phosphonate (DMnHP) at B3LYP/def2-TZVP level. Color code: orange ball is phosphorus, red balls are oxygen, gray balls are carbon, and white balls are hydrogen atoms.
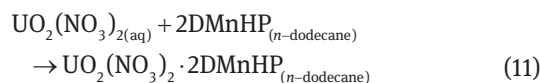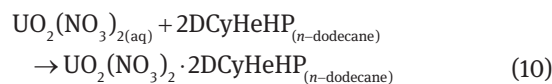
and DMnHP. A number of different starting geometric configurations were considered for the ligands (eight for DCyPeHP and five each for DCyHeHP and DMnHP), and are subjected to geometry optimization at B3LYP/def2-TZVP level. The lowest energy geometries for the ligands are represented in Figure 11a–c.

The Mulliken population analysis shows considerable amount of positive charge on the phosphorus atom (~0.71e) and negative charge concentration on P=O oxygen (−0.53e). After establishing the ground state geometry of the ligands, we have investigated their complexation behavior with $UO_2(NO_3)_2$. Seven starting geometries were generated for each complexes, namely $UO_2(NO_3)_2 \cdot 2DCyPeHP$, $UO_2(NO_3)_2 \cdot 2DCyHeHP$, and $UO_2(NO_3)_2 \cdot 2DMnHP$, by distributing the ligands and nitrates around UO_2 unit in all possible ways. The energetically lowest-lying geometries corresponding to each metal complex are represented in Figure 12a–c, respectively. In all three complexes, nitrate groups are localized on the equatorial region of the O=U=O axis, and are slightly tilted from the equatorial plane. The ligand units are oriented trans to each other with average U–O (ligand) distance of 2.39–2.41 Å and U=O bond length of 1.75 Å.

Our recent theoretical studies on the extraction behavior of TBP indicated that the effectiveness of extraction by a particular ligand can be directly correlated to the computed extraction energy [38]. In this regard, we have evaluated the extraction energy for the respective complexes as the energy balance of the following equations.

$$UO_2(NO_3)_{2(aq)} + 2DCyPeHP_{(n-dodecane)}$$
$$\rightarrow UO_2(NO_3)_2 \cdot 2DCyPeHP_{(n-dodecane)} \quad (9)$$

$$UO_2(NO_3)_{2(aq)} + 2DCyHeHP_{(n-dodecane)}$$
$$\rightarrow UO_2(NO_3)_2 \cdot 2DCyHeHP_{(n-dodecane)} \quad (10)$$

$$UO_2(NO_3)_{2(aq)} + 2DMnHP_{(n-dodecane)}$$
$$\rightarrow UO_2(NO_3)_2 \cdot 2DMnHP_{(n-dodecane)} \quad (11)$$

Before the extraction, the $UO_2(NO_3)_2$ species are in the aqueous medium whereas the ligands (DCyPeHP, DCyHeHP and DMnHP) are in n-dodecane environment. Upon extraction, the respective metal-ligand complexes that are formed at the aqueous organic interface and are extracted into the n-dodecane + extractant medium. Due to this fact, the actual solvent environment of the metal complex is n-dodecane + extractant. However, in the present study, we have approximated
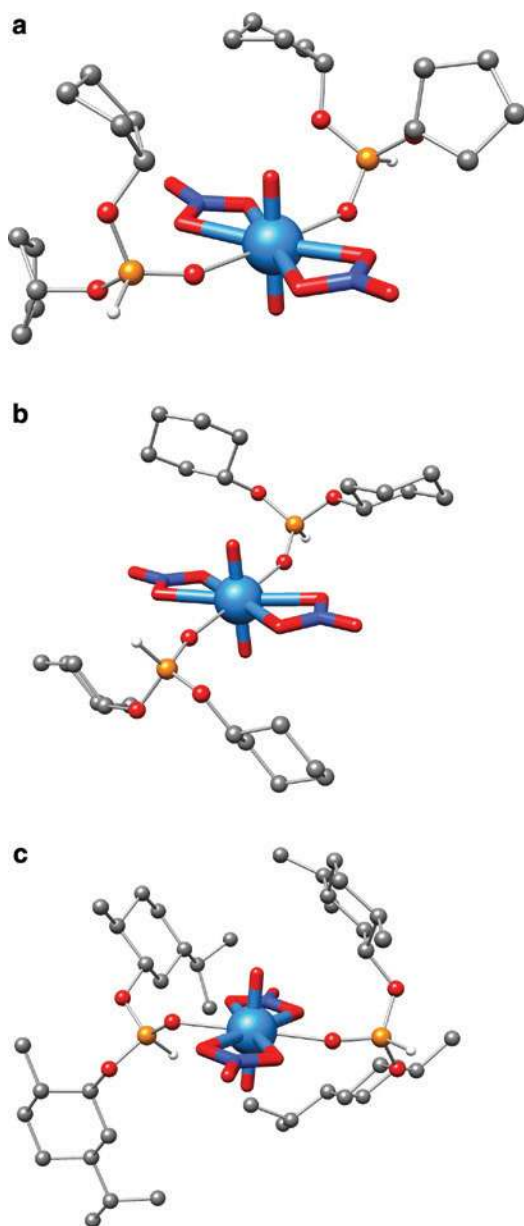
Figure 12: Optimized geometries of (a) $UO_2(NO_3)_2 \cdot 2DCyPeHP$; (b) $UO_2(NO_3)_2 \cdot 2DCyHeHP$ and (c) $UO_2(NO_3)_2 \cdot 2DMnHP$ at PBE0/def2-TZVP-ECP level. Hydrogen atoms are omitted from cyclopentyl and cyclohexyl rings for clarity, and uranium atom is represented using blue color. Please refer to the caption of Figure 11 for color code.

the solvent environment as *n*-dodecane, as we were not able to measure the dielectric constant of the *n*-dodecane + extractant mixture. The influence of the solvent environment was considered by performing single point calculations on the optimized geometries with the conductor-like screening model (COSMO)[39] (dielectric constant of aqueous phase, $\varepsilon = 80.4$, and *n*-dodecane $\varepsilon = 2$) at PBE0/def2-TZVP-ECP level. It is to be noted that the computed complexation energies (where all the species in equations

9, 10 and 11 are considered in gas phase), are -71.6, -73, and -88.4 kcal/mol, respectively for $UO_2(NO_3)_2 \cdot 2DCyPeHP$, $UO_2(NO_3)_2 \cdot 2DCyHeHP$ and $UO_2(NO_3)_2 \cdot 2DMnHP$. This trend is in agreement with the trend observed experimentally. The calculated extraction energies are -56.4, -55.8, and -71.6 kcal/mol for $UO_2(NO_3)_2 \cdot 2DCyPeHP$, $UO_2(NO_3)_2 \cdot 2DCyHeHP$, and $UO_2(NO_3)_2 \cdot 2DMnHP$, respectively. It is interesting to observe that the difference in extraction energies between $UO_2(NO_3)_2 \cdot 2DCyPeHP$ and $UO_2(NO_3)_2 \cdot 2DMnHP$ is 15.2 kcal/mol, which is of the order of 15.5 kcal/mol energy difference estimated for TBP with $Pu(NO_3)_4 \cdot 2TBP$ and $Zr(NO_3)_4 \cdot 2TBP$ [35]. On the other hand, the extraction energies of $UO_2(NO_3)_2 \cdot 2DCyPeHP$ and $UO_2(NO_3)_2 \cdot 2DCyHeHP$ are very much similar and does not clearly corresponds to their experimentally observed trend in extraction behavior. The evaluated large extraction energy of $UO_2(NO_3)_2 \cdot 2DMnHP$ indicates the preference of DMnHP ligands for $UO_2(NO_3)_2$ species and is in agreement with our observed trend in distribution ratios.

4 Conclusions

A new class of alicyclic H-phosphonates, namely, dicyclopentyl H-phosphonate (DCyPeHP), dicyclohexyl H-phosphonate (DCyHeHP) and dimenthyl H-phosphonate (DMnHP), were synthesized and characterized by various spectroscopic and analytical techniques. The synthesis of extractants was carried out using commercially available materials in single step with high yields and purity. These compounds extract actinides through P–OH group which is present in tautomeric equilibrium with the P–H bond at lower acidities and by solvation mechanism at higher acidities through phosphoryl oxygen. Dimenthyl H-phosphonate showed excellent extraction behavior over dicyclopentyl H-phosphonate, dicyclohexyl H-phosphonate for actinides. Density functional theory calculations were applied to understand the electronic structure of the ligands DCyPeHP, DCyHeHP and DMnHP and their corresponding metal complexes with $UO_2(NO_3)_2$. Based on our calculations we were able to derive lowest energy geometries for the ligands and metal complexes. In all three metal complexes, the ligands are distributed -trans to each other and the nitrate groups are localized on the equatorial region of the O=U=O axis. The computed complexation energies are -71.6, -73, and -88.4 kcal/mol, respectively for $UO_2(NO_3)_2 \cdot 2DCyPeHP$, $UO_2(NO_3)_2 \cdot 2DCyHeHP$, and $UO_2(NO_3)_2 \cdot 2DMnHP$. The computed large complexation energy of $UO_2(NO_3)_2 \cdot 2DMnHP$ suggests the preference of DMnHP ligands for $UO_2(NO_3)_2$ species, in agreement with our observed experimental data.

References

1. Nash, K. L., Lumetta, G. J.: Advanced separation techniques for nuclear fuel reprocessing and radioactive waste treatment. Elsevier, Woodhead Publishers, Cambridge (2011).
2. Lawrosky, S.: Survey of separation processes other than solvent extraction. Chem. Eng. Prog. **51**, 461 (1955).
3. Grebenshchikova, V., Bryzgalova, R.: A study of the co-precipitation of Pu (IV) with lanthanum oxalate. Radiokhimia **2**, 265 (1960).
4. Korkisch, J., Worsfold, P.: Handbook of ion exchange resins: their application to inorganic analytical chemistry: Volume 1, CRC Press, Boca Raton, FL, 1989. Anal. Chim. Acta **236**, 511 (1990).
5. Artyushin, O., Sharova, E., Odinets, I., Lenevich, S., Morgalyuk, V., Tananaev, I., Pribylova, G., Myasoedova, G., Mastryukova, T., Myasoedov, B.: Simple route to secondary amides of phosphorylacetic acids and their use for extraction and sorption of actinides from nitric acid solutions. Russ. Chem. Bull. **53**, 2499 (2004).
6. Singh, S. K., Tripathi, S., Singh, D.: Studies on the separation and recovery of uranium from phosphoric acid medium using a synergistic mixture of (2-ethylhexyl) phosphonic acid mono 2-ethyl hexyl ester (PC-88A) and tri-n-octylphosphine oxide (TOPO). Sep. Sci. Technol. **45**, 824 (2010).
7. Karve, M., Gaur, C.: Liquid-liquid extraction of Th (IV) with Cyanex302. J. Radioanal. Nucl. Chem. **270**, 461 (2006).
8. Maiorov, V., Nikolaev, A., Adkina, O., Mazunina, G.: Extraction of thorium with tributyl phosphate from chloride solutions. Radiochemistry **48**, 576 (2006).
9. Coleman, C., Brown, K., Moore, J., Crouse, D.: Solvent extraction with alkyl amines. Ind. Eng. Chem. **50**, 1756 (1958).
10. Schulz, W. W., Burger, L. L., Navratil, G. D., Bender, K. P.: Science and technology of tri butyl phosphate, applications of tributyl phosphate in nuclear fuel reprocessing. Vol. 3 (1990), CRC Press, Boca Raton, Florida, p. 2.
11. Kalina, D. G., Philip Horwitz, E.: Variations in the solvent extraction behavior of bifunctional phosphorus-based compounds modified with TBP. Solvent Extr. Ion Exch. **3**, 235 (1985).
12. Corbridge, D. E. C.: Phosphorus-an outline of its chemistry, biochemistry and technology. Elsevier Science Publishers, Amsterdam (1985).
13. Feng, C.-G., Ye, M., Xiao, K. J., Li, S., Yu, J. Q.: Pd (II)-catalyzed phosphorylation of aryl C–H bonds. J. Am. Chem. Soc. **135**, 9322 (2013).
14. Rulev, A. Y.: Recent advances in Michael addition of H-phosphonates. RSC Adv. **4**, 26002 (2014).
15. Brahmmananda Rao, C.V.S., Jayalakshmi, S., Subramaniam, S., Sivaraman, N., Vasudeva Rao, P.R: Extraction studies of actinides and lanthanides by bifunctional H-phosphonates. Radiochim. Acta. **103**, 345 (2015).
16. Fakhraian, H., Mirzaei, A.: Reconsideration of the base-free batch-wise esterification of phosphorus trichloride with alcohols. Org. Process Res. Dev. **8**, 401 (2004).
17. Sindhu, P.: Practicals in physical chemistry. Macmillan Publishers, India (2005).
18. Ihle, H., Karayannis, M., Murrenhoff. A.: Organic scintillators and liquid scintillation counting (1971), Academic Press, New York, p. 879.
19. Becke, A. D.: Density-functional thermochemistry. III. The role of exact exchange. J. Chem. Phys. **98**, 5648 (1993).
20. Lee, C., Yang, W., Parr, R. G.: Development of the Colle-Salvetti correlation-energy formula into a functional of the electron density. Phys. Rev. B **37**, 785 (1988).
21. Schafer, A., Horn, H., Ahlrichs, R.: Fully optimized contracted Gaussian basis sets for atoms Li to Kr. J. Chem. Phys. **97**, 2571 (1992).
22. Weigend, F., Ahlrichs, R.: Balanced basis sets of split valence, triple zeta valence and quadruple zeta valence quality for H to Rn: design and assessment of accuracy. PCCP **7**, 3297 (2005).
23. Sousa, S. F., Fernandes, P. A., Ramos, M. J.: General performance of density functional. J. Phys. Chem. A. **111**, 10439 (2007).
24. Tirado-Rives, J., Jorgensen, W. L.: Performance of B3LYP density functional methods for a large set of organic molecules. J. Chem. Theory Comput. **4**, 297 (2008).
25. Weigend, F.: A fully direct RI-HF algorithm: implementation, optimised auxiliary basis sets, demonstration of accuracy and efficiency. PCCP **4**, 4285 (2002).
26. Weigend, F., Köhn, A., Hättig, C.: Efficient use of the correlation consistent basis sets in resolution of the identity MP2 calculations. J. Chem. Phys. **116**, 3175 (2002).
27. Sierka, M., Hogekamp, A., Ahlrichs, R.: Fast evaluation of the Coulomb potential for electron densities using multipole accelerated resolution of identity approximation. J. Chem. Phys. **118**, 9136 (2003).
28. Grimme, S., Ehrlich, S., Goerigk, L: Effect of the damping function in dispersion corrected density functional theory. J. Comput. Chem. **32**, 1456 (2011).
29. Grimme, S., Antony, J., Ehrlich, S., Krieg, H.: A consistent and accurate ab initio parametrization of density functional dispersion correction (DFT-D) for the 94 elements H-Pu. J. Chem. Phys. **132**, 154104 (2010).
30. Adamo, C., Barone, V.: Toward reliable density functional methods without adjustable parameters: the PBE0 model. J. Chem. Phys. **110**, 6158 (1999).
31. Greif, A. H., Hrobarik, P., Autschbach, J., Kaupp, M.: Giant spin-orbit effects on ^{1}H and ^{13}C NMR shifts for uranium (VI) complexes revisited: role of the exchange-correlation response kernel, bonding analyses, and new predictions. Phys. Chem. Chem. Phys. **18**, 30462 (2016).
32. Kuchle, W., Dolg, M., Stoll, H., Preuss, H.: Energy-adjusted pseudopotentials for the actinides. Parameter sets and test calculations for thorium and thorium monoxide. J. Chem. Phys. **100**, 7535 (1994).
33. Cao, X., Dolg, M.:Valence basis sets for relativistic energy-consistent small-core lanthanide pseudopotentials. J. Chem. Phys. **115**, 7348 (2001).

34. Cao, X., Dolg, M.: Segmented contraction scheme for small-core actinide pseudopotential basis sets. J. Mol. Struct. **673**, 203 (2004).

35. Neese, F.: The ORCA program system. Wiley Interdiscip. Rev. Comput. Mol. Sci. **2**, 73 (2012).

36. Katcyuba, S. A., Monakhova, N. I., Ashrafullina, L. K., Shagidullin, R. R.: Vibrational spectra, conformations and force constants of dialkylphosphites. J. Mol. Struct. **269**, 1 (1992).

37. Das, D., Goud, E., Annam, S., Jayalakshmi, S., Gopakumar, G., Brahmmananda Rao, C. V. S., Sivaraman, N., Sivaramakrishna, A., Vijayakrishna, K.: Experimental and theoretical studies on extraction behavior of di-n-alkyl phosphine oxides towards actinides. RSC Adv. **5**, 107421 (2015).

38. Gopakumar, G., Sreenivasulu, B., Suresh, A., Brahmmananda Rao, C. V. S., Sivaraman, N., Joseph, M., Anoop, A.: Complexation behaviour of tri-n-butyl phosphate ligand with Pu (IV) and Zr (IV): a computational study. J. Phys. Chem. A. **120,** 4201 (2016).

39. Klamt, A., Schüürmann, G.: A new approach to dielectric screening in solvents with explicit expressions for the screening energy and its gradient. J. Chem. Soc., Perkin Trans. **2**, 799 (1993).